Volumes of Dam Material Mobilized by Erosion During Tailings Dam Failure Events

Daniel Adria, Knight Piésold, Canada
Violeta Martin, Knight Piésold, Canada
Heleman Wong, Knight Piésold, Canada

Abstract

The breach size and shape, and the rate at which it is formed, are key characteristics that must be estimated for conducting a dam breach analysis. A frequently used simplification in such analysis is that the breach channel through a dam is trapezoidal in cross section. This convention allows for consistent comparison between historical dam breaches (water and tailings dams alike) and is useful for numerical modelling of the breach hydrograph and downstream flood wave or runout propagation. However, a breach channel is three-dimensional, and an assessment of the volume of the dam material mobilized for a given two-dimensional trapezoidal breach geometry represents an additional useful parameter to consider when conducting the breach analysis.

The breach geometry and the mobilized dam volumes in a tailings dam breach event could vary substantially depending on the construction type, the dam geometry, and the construction materials used. The breach characteristics can also be impacted by the breach mechanism, which appears to be different for erosional type mechanisms (i.e., overtopping and internal erosion) compared to non-erosional type mechanisms (e.g., slope instability, foundation failure, liquefaction). It is important to include such considerations when conducting tailings dam breach analyses, as they may present physical constraints for the breach development.

Two empirical equations for calculating the eroded dam volume and the dam erosion rate are presented in this paper. Multiple linear regression equations were developed for a combination of historical erosional breach events of water and tailings dams, which use the breach height and the breach outflow volume as inputs. Also presented is a method to estimate whether the supernatant pond volume is sufficiently large for an erosional breach to progress to the foundation based on these equations.

Introduction

The breach size and shape, and the rate at which it is formed, are the key characteristics that must be estimated when conducting a tailings dam breach analysis (TDBA). A frequently used simplification is that the breach channel through a dam is trapezoidal in cross section. This convention allows for consistent comparison between historical dam breaches (water and tailings dams alike) and is useful for numerical modelling of the breach hydrograph and downstream flood wave or runout propagation using the parametric breach approach (Froehlich, 2008; Wahl, 1998). The parametric breach approach is available in commonly used software for TDBAs (e.g., HEC-RAS, FLO-2D, RiverFlow2D). Many empirical equations developed for water retaining dam breaches use this convention as well.

A breach channel is three-dimensional, however, and an assessment of the volume of the dam material mobilized for a given two-dimensional trapezoidal breach geometry represents an additional useful parameter to consider when conducting the breach analysis. The breath or thickness of tailings dams can range substantially between facilities and dam construction methods (e.g., upstream, centerline, or downstream). All else being equal, it is intuitive that a larger breach channel would develop in a narrower upstream or centerline constructed dam compared to a wider downstream constructed dam (Figure 1), as the same amount of energy would be available for eroding through a much larger dam volume.

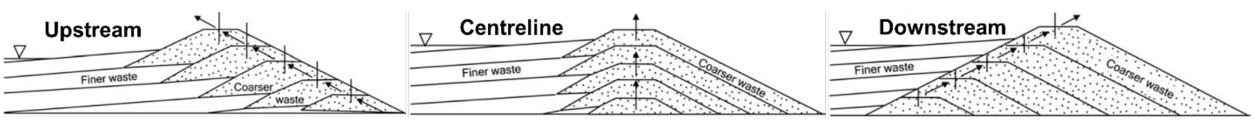

Figure 1: Comparison of tailings dam geometries (adapted from Blight, 2010)

Despite this, most common empirical equations would suggest the same formation time and breach width for both tailings dams, which limits the inclusion of either adverse or favorable site-specific conditions such as the dam size and geometry. Furthermore, these empirical equations are not appropriate to use when the failure is caused by non-erosional mechanisms (e.g., slope instability, foundation failure, liquefaction, etc.), because they were developed for overtopping and internal erosion type failures. The outflow volume, breach geometry and formation time, as well as the peak flow and hydrograph shape are strongly impacted by whether a dam is breached through erosional or non-erosional mechanisms, as discussed in this paper.

Adria et al. (2023a) presented a paper at the 2023 Canadian Dam Association (CDA) conference, in which they introduced two empirical equations for calculating the eroded dam volume and the dam erosion rate for erosional breach scenarios. While these equations are applicable to both water and tailings dams, their applicability to tailings dams and some of the examples presented in that paper are further discussed herein. These examples include specific considerations such as a method to estimate whether the supernatant pond volume is sufficiently large for an erosional breach to progress to the foundation. Additional work is ongoing to expand on the understanding and the dataset related to erosional breaches of tailings dams.

Dam breach processes

Deep understanding of the physical processes during the breach and subsequent flood wave propagation are key requirements for conducting successful breach studies (Rana et al., 2021a). For context within this paper, these processes and existing conventions are summarized below.

Breach geometry conventions

The breach geometry is typically represented with a trapezoid (Figure 2), using the breach height, the average breach width (B_{Avg}), and the breach side slopes (Z_L and Z_R). The bottom breach width (B_B), or alternatively the top breach width (B_T) could be used. The ultimate breach geometry for erosional breaches can be formed by a V-shape cut that progresses downwards until it encounters materials that are substantially less erodible than the dam material, after which it starts widening until the outflow no longer has the capacity to further enlarge the breach opening. The period from when the V-shape begins cutting down into the dam to when the ultimate breach geometry is reached is considered the breach formation time. The formation time excludes the comparatively minor head-cutting phase that occurs during the initial overtopping or internal erosion development (Wahl, 1998), prior to the main breach progression. The breach geometry for non-erosional breaches appear to have more rounded shapes (e.g., U-shapes), but could be reasonably approximated with the same trapezoidal convention (Adria et al., 2023b).

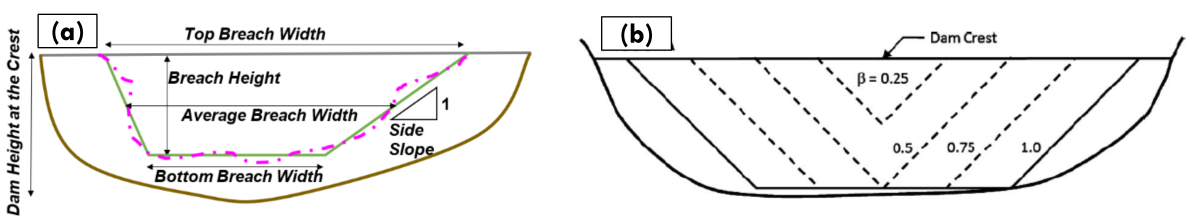

Figure 2: Trapezoidal breach: a) geometry and b) breach formation (Froehlich, 2008)

Breach and outflow processes

Breach processes and characteristics developed through internal erosion and overtopping of water retaining dams are well understood and documented (e.g., USBR, 1988; Wahl, 1998; Froehlich, 2008; Wahl, 2014; Walsh et al., 2021). These processes primarily involve erosion of the dam materials by water flowing over the crest or through the dam over a period of minutes to hours. Failures can also be caused by slope instability, foundation failure, structural failure, liquefaction, or other mechanisms that could remove the containment structure within seconds to minutes. In such "non-erosional" type failures, erosion does not play a key role, as these failures are dominated by geotechnical characteristics (e.g., slip surfaces, residual undrained shear strength ratios, etc.) rather than pond volumes.

The breach outflow volume for tailings dam breaches depends on whether there is a pond present in the TSF, and whether the tailings are susceptible to liquefaction (Small et al., 2017; CDA, 2021). The CDA

TDBA guidelines (2021) further identify two processes to qualitatively describe the discharge mechanisms associated with the outflow of the supernatant pond and/or flowable tailings. Process I is the discharge of the supernatant pond that carries tailings and dam materials mobilized through erosion, which can often be analyzed using Newtonian fluid approximations. Process II is the outflow of flowable tailings that are mobilized due to liquefaction or progressive slumping of unsupported tailings until a stable tailings slope is achieved (backscarp). The outflow from Process II would be primarily comprised of tailings solids and interstitial water, and therefore would have a much lower water content (i.e., higher solids content) compared to Process I. Process II outflows must be analyzed using non-Newtonian fluid approximations and associated rheological properties for the tailings material. A breach can, but does not have to, include both Process I and Process II outflows, which can occur in either order, or simultaneously.

As the breach opening develops and the outflows propagate downstream, the physical impacts of the two discharge mechanisms typically are notably different. Process I breach outflows have a relatively low solids content and are highly erosive, as was observed in the Mount Polley failure in 2014 with the erosion of Hazeltine Creek (Morgenstern et al., 2015; Cuervo et al., 2017). In contrast, Process II runouts have a high solids content and typically result in limited erosion. For example, the liquefied tailings outflow from the Prestavèl TSF in Italy (i.e., Stava) had a high fluidity and an intensive destructive power, but the downstream creek channel itself did not undergo much erosion or deposition (Berti et al., 1988). Takahashi (2014) stated that no erosion occurred because the solids fraction inside the water-sediment mixture of the Prestavèl tailings was so high (approximately 48% by volume) that the flow could not become denser through additional erosion. Hungr et al. (2005) similarly stated that flows with lower sediment concentrations can be expected to be more erosive than flows with higher sediment concentrations.

In this paper, the focus is on erosional breach processes through the embankment, which is considered separate from the downstream erosion of stream-channels and their floodplains.

Development of eroded dam volume equations

Adria et al. (2023a) developed two empirical equations to estimate the eroded dam volume (V_{ED}) and the mean eroded dam volume rate (M), which make use of the combined and verified databases for water retaining dam breaches from Wahl (1998, 2014) and erosional tailings dam breaches from Adria et al. (2023b). The proposed relationships are based on multiple linear regressions (MLRs) of dam height and outflow volume. MLRs have better predictive capabilities than the methods in which each input is used individually or combined (as in the height-volume product in MacDonald and Langridge-Monopolis, 1984). The two MLR equations are defined as follows:

$$V_{ED} = 1.26 H_W{}^{1.803} V_{Out}{}^{0.338} \tag{1}$$

$$M = \frac{V_{ED}}{T_f} = 415\, H_W{}^{2.296} V_{Out}{}^{-0.098} \tag{2}$$

In these equations V_{ED} is the volume of the eroded dam material [m³], H_w is the height of water above the breach [m], V_{Out} is the volume of breach outflow that typically includes the supernatant pond and the eroded tailings material [m³], M is the mean eroded dam volume rate [m³/hr], and T_f is the breach formation time [hr]. The variable V_{ED} is the same as V_M or V_{Er} used by MacDonald and Langridge-Monopolis (1984) or Wahl (1998), however, the labelling is changed to prevent confusion with eroded tailings volumes, or dam materials that mobilize through non-erosional breach processes. The events used to develop the empirical equations are compiled in Tables A1 and A2 of the Appendix to this paper.

Figure 3, reproduced from Adria et al. (2023), compares the predicted values for: (a) the eroded dam volume using Equation 1, and (b) the mean eroded dam volume rate using Equation 2 with observed values, while the insets show a box and whisker plot of the predicted to observed ratios. The dashed lines represent half an order of magnitude above and below the 1:1 line, indicating the approximate range of the error. Ideally, the boxplots have a mean and median close to unity (indicating little error on average) and a narrow interquartile range (indicating lower variability in estimated value accuracy). The interquartile ranges for the two equations are comparable to or are smaller than observed in earlier equations, indicating good predictive ability (Wahl, 2004).

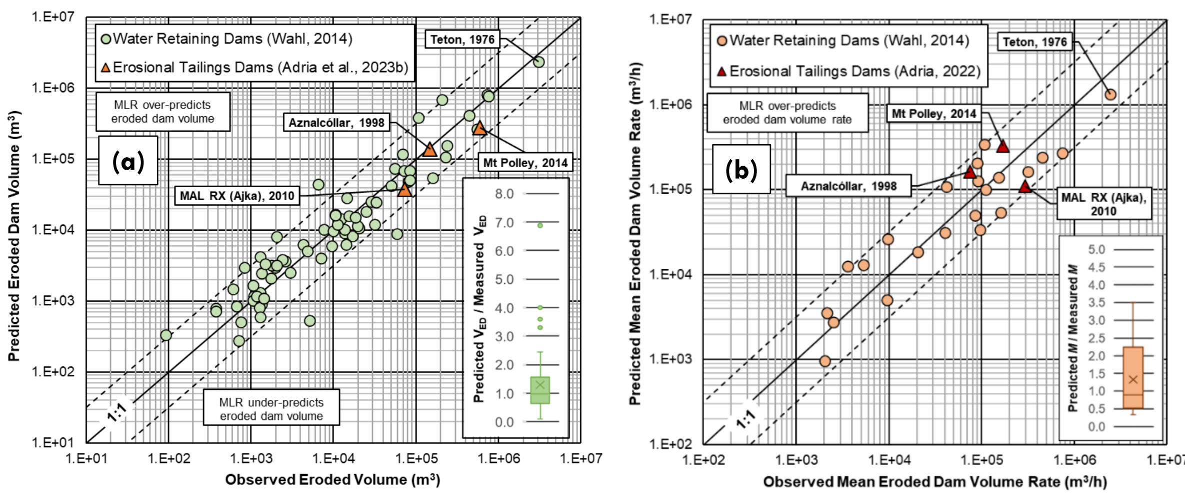

Figure 3: Comparison of observed and predicted values for: (a) eroded dam volume, and (b) mean eroded dam volume rate (from Adria et al., 2023)

For Equations 1 and 2, the volume of tailings that are eroded with the supernatant pond during Process I outflows is included in V_{Out}, while the liquefied tailings volume discharged in Process II outflows is not included in V_{Out} in consideration of the limited erosive potential of Process II flows (this can be changed depending on project-specific conditions). Equations 1 and 2 are not meant to be applied to non-erosional breach events, for which the breach develops due to drivers other than erosion. For the tailings dam breach events that were included in the development of regression equations shown in Figure 3, the estimated volumes of tailings eroded during the supernatant pond discharge (i.e. Process I) were included in the analysis. A Process II outflow volume may be estimated separately after the breach geometry is selected, and the runout from Process II either evaluated separately or included in the final outflow hydrograph, as appropriate for the project-specific conditions.

The eroded dam volume rate varies during the breach development, with higher rates occurring during the peak outflow and lower rates during the rising and receding limbs of the breach hydrograph. The value predicted by Equation 2 represents the average or the mean rate. The mean eroded dam volume rate itself cannot be used as an input for most dam breach hydrograph modelling approaches, but needs to be combined with an estimate of the eroded dam volume to inform the breach formation time. The eroded dam volume can be estimated either by using Equation 1, or by using other regression equations to determine the breach width and side slopes (e.g., Froehlich, 2008; Xu and Zhang, 2009), and then converted to the eroded dam volume using relatively simple geometric equations. The Washington Guidelines (2007) include discussion on these geometric equations, or 3D CAD modelling can also be used to calculate the eroded dam volume based on the estimated breach geometry for more complex dam geometries if required (e.g., buttresses, or varying slopes). The primary advantage of estimating the mean eroded dam volume rate is to support the selection of both the breach geometry and the breach formation time.

Applications of eroded dam volume equations to tailings dams

Adria et al. (2023a) presented several examples that illustrate the impact of outflow volume or dam geometry on the breach size or the rate of breach development. They also included examples to demonstrate how topographic constraints may impact the breach development, and a discussion on how to use sensitivity analysis to support the final selection of breach parameters. Some of those examples relevant to tailings dams are included herein.

Determining breach widths and breach heights

Breach analysis ideally considers the dam geometry in a rational, non-subjective way. The characteristics of three TSFs that are 50 m tall are summarized in Table 1. These TSFs are hypothetical, but the geometries and pond volumes are comparable with the range the authors have observed for real TDBAs. TSF 1 and TSF 2 have the same pond volume, but TSF 1 has a thinner geometry (i.e., smaller crest width, steeper downstream slope, and a centerline dam construction with nearly vertical upstream slope). TSF 2 and TSF 3 are both downstream constructed dams with the same dam geometry, but the supernatant pond volumes are different. The tailings are considered non-liquefiable (i.e., they would represent Case 1B according to CDA, 2021); however, a portion of the tailings would be eroded and mobilized during the breach development. The eroded tailings volume in Process I was calculated using a 30% volumetric solids concentration in the outflow and a void ratio of 1 for the tailings material (Fontaine and Martin, 2015; CDA, 2021).

In Table 1, Equation 1 was used to calculate the Eroded Dam Volume for all three dams, which was then used to estimate the breach height and the bottom width given the outflow volume. The assumed breach side slopes for all three dams are 1H:1V. TSF 1 and TSF 2 are used to demonstrate how Equation 1 can be used to quantitatively consider the dam geometry (i.e., the dam thickness), rather than relying on subjective adjustments to empirical equation results. For both TSFs the same volume of dam material is predicted to erode (as the pond volumes, and thus, the breach outflow volumes, V_{Out}, are identical); however, the breach width for the downstream constructed dam must be narrower to erode the same dam volume given the same breach height.

Table 1: Comparison of estimated breach heights for different TSF characteristics

Parameter	TSF 1: Large pond centerline dam	TSF 2: Large pond downstream dam	TSF 3: Small pond downstream dam
Supernatant Pond Volume (m^3)	1,800,000	1,800,000	400,000
Eroded Tailings Volume (m^3)	2,700,000	2,700,000	600,000
Total Outflow Volume (m^3)	4,500,000	4,500,000	1,000,000
Crest Width (m)	5	20	20
Upstream and Downstream Slopes (xH:1V)	0 and 2	1 and 4	1 and 4
Calculated Eroded Dam Volume (m^3)	258,000	258,000	62,000
Calculated Breach Height (m)	50	50	30
Calculated Breach Bottom Width (m)	60	0	0

The second pair of TSFs (TSF 2 and TSF 3) that have different supernatant pond volumes is used to demonstrate the relationship between the breach outflow volume and the possible breach height to reach the predicted eroded dam volume from Equation 1. In this process, the breach height can be determined as follows:

1. The required volume of the dam that must be eroded for a breach to reach a given elevation is calculated using the geometric relation between breach geometry and eroded dam volume as per the Washington Guidelines (2007). The breach geometry uses a breach side slope of 1H:1V (or alternate as selected), a bottom breach width of 0, and a given dam geometry (i.e., crest width, upstream dam slope, and downstream dam slope). The calculation is performed at regular breach depth intervals, moving downwards from the crest elevation, to represent a V-shape erosion progression from Froehlich (2008).

2. The potential eroded dam volume that could be eroded for each breach height is calculated using Equation 1 for the same intervals using the predetermined outflow volume and varying the breach height.
3. The two eroded dam volume curves are plotted, and the breach elevation where the required eroded dam volume (Step 1) exceeds the potential eroded dam volume (Step 2) (i.e., the intersection of the two curves) represents the ultimate breach height. If the two curves do not intercept, the breach could progress down to natural ground.

This process is shown in Figure 4 (reproduced from Adria et al., 2023), using the hypothetical example of TSF 2 and TSF 3 from Table 1. The eroded dam volumes are placed on the x-axis to align the breach elevation (y-axis) vertically with the breach geometry schematic; the eroded dam volume remains as the independent variable in this procedure. The small pond is unable to erode the dam to its foundation, while the large pond is sufficient to erode it to the foundation. A pond larger than 1,800,000 m^3 would be able to erode the downstream constructed dam to foundation and proceed to lateral erosion and breach widening, as described by Froehlich (2008). Dam features that also could arrest breach should be identified to support an estimated breach elevation that is above the foundation elevation. For example, a large buttress or bench is a plausible cause for the vertical breach progression to be slowed or stopped.

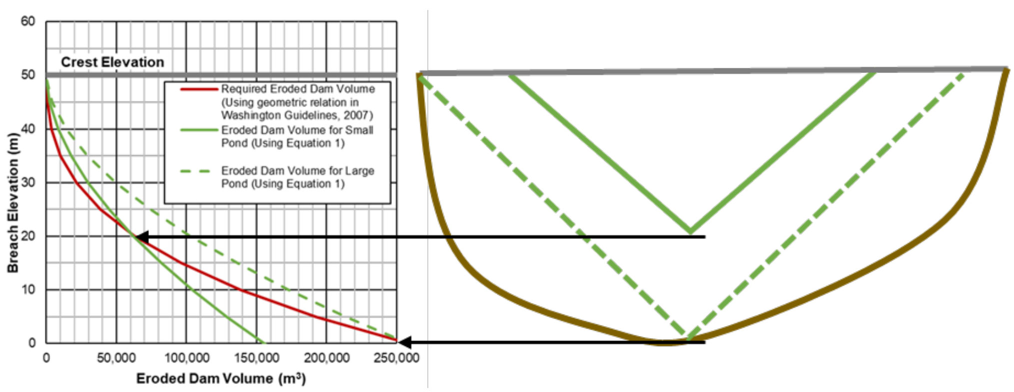

Figure 4: Comparison of the calculated eroded dam volume against the dam volume that would need to be eroded to reach a specific breach height with the V-shape breach

Refining formation times for sensitivity scenarios

A practitioner may ultimately choose more conservative inputs than what is estimated from any one regression equation; however, the combination of these conservative choices should remain within reason, which can be supported using the mean dam erosion rate equation. A larger breach, faster breach, or a combination of a larger and a faster breach could be assessed; however, these scenarios could result in physically impossible and extreme breach outflows. By using Equation 2 and the scatter in Figure 3b, an upper and lower bound on the mean eroded dam volume rate can be estimated for the sensitivity scenarios.

Using TSF 1 from Table 1 as an example, a breach bottom width and a breach formation time were estimated for the base case using Froehlich (2008). The values selected for the sensitivity scenarios (wide or fast breach) were based on the results from Froehlich (2008), and adjusted using the error guidance for these parameters from Wahl (2004). The selected breach side slope for this example was 1H:1V. The example results are shown in Table 2 (from Adria et al., 2023), where the breach width and formation time were calculated using Froelich (2008), V_{ED} was calculated using the geometric relations in Washington Guidelines (2007), and *M* was calculated using the dam breach formation time from Froehlich (2008) and the eroded dam volume from Washington Guidelines (2007).

Table 2: Mean eroded dam volume rates for sensitivity scenarios for a centerline dam

Parameter	Base Case	Wide Breach	Fast Breach	Wide and Fast Breach
Average Breach Width (m)	55	110	55	110
Bottom Breach Width (m)	5	60	5	60
Breach Formation Time (hr)	0.24	0.24	0.12	0.12
Eroded Dam Volume (m^3)	110,000	260,000	110,000	260,000
Eroded Dam Volume Rate (m^3/hr)	458,000	1,080,000	917,000	2,170,000

In comparison, Equation 2 predicts a mean eroded dam volume rate of 736,000 m^3/h. The maximum error for Equation 2 is approximately 0.5 orders of magnitude, therefore the maximum and minimum *M* values could be as high as 2,327,000 m^3/h and as low as 233,000 m^3/h, respectively. The base case values, as predicted using Froehlich (2008), result in an *M* value that is less than the predicted value from Equation 2. This is due to the implicit assumption in Froehlich (2008) that the dam would be downstream constructed and would have more dam material that could be eroded during a breach. A simple change from a centerline dam to a downstream dam that has an upstream dam slope of 2H:1V would result in a similar *M* value when using Froehlich (2008) to that calculated using Equation 2.

The wide breach and fast breach scenarios have an *M* value (i.e., 1,080,000 m^3/hr and 917,000 m^3/hr) that is between the best estimate and the maximum *M* value from Equation 2 (i.e., 736,000 m^3/hr and 2,327,000 m^3/hr, respectively) for the example dam. The wide and fast breach scenario has an *M* (2,170,000 m^3/hr) that is about the same as the maximum *M* value from Equation 2. The adjustments in the breach width and formation time used for these hypothetical sensitivity cases are not extreme and are less than the typical uncertainties when using multiple empirical equations (Adria et al., 2023a) but result in an extreme outcome when combined. Depending on the project-specific conditions, the wide and fast breach sensitivity scenario may not be physically possible, or it could be representative of a worst-case scenario for an erosional breach.

It is noted that credible non-erosional breach scenarios could still result in a wider and faster breach than a worst-case erosional breach; however, it is also possible that a non-erosional breach is smaller than the erosional breach and may not represent the worst-case scenario (e.g., a decapitation or a shallow surface slip type failure).

Comparisons to case histories

There are numerous uncertainties in TDBAs every step along the way. It is therefore prudent and beneficial to compare the final selection of breach parameters against case histories to assess whether the selections are reasonable and sufficiently conservative. To assess the predicted mobilized tailings volume in a TDBA, the outflow volume can be compared to the impounded volume. This comparison is shown in Figure 5 (reproduced from Adria et al., 2023), which is adapted from Rana et al. (2021a and 2021b).

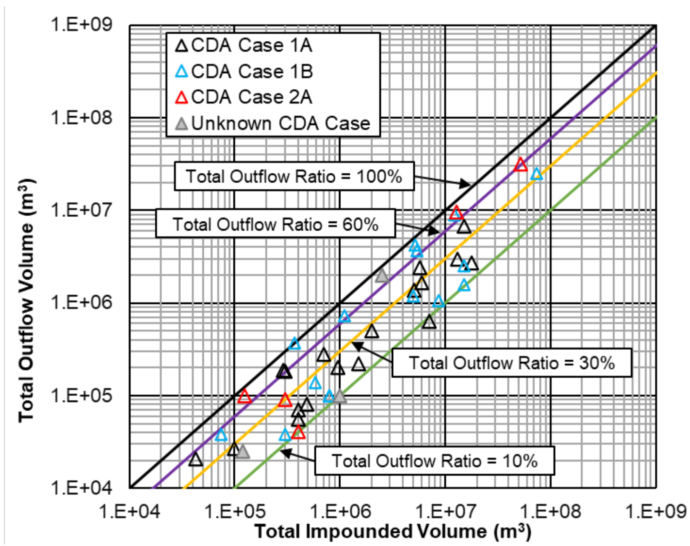

Figure 5: Total outflow ratios for past tailings dam failures (adapted from Rana et al., 2021a)

Other types of comparisons are shown in the Appendix and include scatter plots of: (A) breach heights to average breach widths, (B) eroded dam volumes, (C) mean erosion rates/breach formation times, and (D) mean dam erosion rates. The plots were developed using data compiled by Wahl (1998, 2014), Walder and O'Connor (1997), Rana et al. (2021b), and Adria et al. (2023b). Colored lines that represent relevant ratios are included on these plots for reference. As an example, if the dam evaluated in the TDBA has a broad geometry and is constructed of erosion-resistant materials, it should plot closer to the lower ratios shown with blue lines on the Appendix figures.

Conclusion

This paper discusses the processes that occur during breach formation that need to be understood to prevent the application of non-analogous case studies or empirical equations to forward-analysis. Two empirical equations from Adria et al. (2023a) are presented that estimate the eroded dam volume and the eroded dam volume rate. These equations can provide additional tools for breach parameter selection, particularly for dam geometries that are outside of the typical conditions in existing dam failure databases. The authors find these equations to be useful tools in their day-to-day practice, as they provide a different measure for checking the reasonableness of the selected breach parameters, given the inherent uncertainties associated with the breach analysis.

Acknowledgements

The authors gratefully acknowledge their clients and colleagues for valuable inputs and support during actual dam breach assessments and preparation of this manuscript. The contributions of Dr Scott McDougall, who collaborated on the CDA 2023 paper, are also greatly appreciated. Various members of the CanBreach Research Program were also instrumental in the development of several key databases used in this paper and contributed thoughtful discussions on several of the themes in this paper over the years. The authors also thank the two reviewers of this manuscript for their constructive comments.-k

References

Adria, D.A.M., Martin, V., McDougall, S., 2023a. The role of sensitivity analysis in selecting dam breach parameters. *Proceedings of the CDA 2023 Annual Conference*, October 22–25, Winnipeg, Canada.

Adria, D.A.M., N. Ghahramani, N.M. Rana, V. Martin, S. McDougall, S.G. Evans and W.A. Take, 2023b. Insights from the compilation and critical assessment of breach and runout characteristics from historical tailings dam failures: Implications for numerical modelling. *Mine Water and the Environment* 42: 650–669. https://doi.org/10.1007/s10230-023-00964-0

Berti, G., F. Villa, D. Dovera, R. Genevois and J. Brauns. 1988. Disaster of Stava, Northern Italy. *Proceedings of the Specialty Conference on Hydraulic Fill Structures:* 492–509.

Blight, G.E. 2010. *Geotechnical Engineering for Mine Waste Storage Facilities*. London, UK: CRC Press/Balkema.

CDA (Canadian Dam Association). 2021. *Technical Bulletin: Tailings Dam Breach Analysis*.

Cuervo, V., L. Burge, H. Beaugrand, M. Hendershot and S.G. Evans. 2017. Downstream geomorphic response of the 2014 Mount Polley tailings dam failure, British Columbia*. Proceedings of the Fourth World Landslide Forum.* Ljubljana, Slovenia. May 29–June 2.

Fontaine, D. and V. Martin. 2015. Tailings mobilization estimates for dam breach studies. *Proceedings of Tailings and Mine Waste 2015,* Vancouver, BC, October 26 to 28: 342–356.

Froehlich, D.C. 2008. Embankment dam breach parameters and their uncertainties. *J Hydraul Eng* 134(12): 1708–1721.

Hungr, O., S. McDougall and M. Bovis. 2005. Entrainment of material by debris flows. *Debris-flow Hazards and Related Phenomena,* M. Jakob and O. Hungr (eds): 135–158. Springer, Berlin.

MacDonald, T.C. and J. Langridge-Monopolis. 1984. Beaching characteristics of dam failures. *J Hydraul Eng* 110(5): 567–586. https://doi.org/10.1061/(ASCE)0733-9429(1984)110:5(567)

Martin, V. and Akkerman, A. Challenges with conducting tailings dam breach assessments. *Proceedings of the International Commission on Large Dams 2017 Annual Meeting, ICOLD,* July 3–7, Prague, Czech Republic (2017).

Morgenstern, N.R., S.G. Vick and D. Van Zyl. 2015. *Independent Expert Engineering Investigation and Review Panel Report on Mount Polley Tailings Storage Facility Breach*

Rana, N.M., N. Ghahramani, S.G. Evans, S. McDougall, A. Small and W.A. Take. 2021a. Catastrophic mass flows resulting from tailings impoundment failures. *Engineering Geology* 292: 106262. https://doi.org/10.1016/j.enggeo.2021.106262

Rana, N.M., N. Ghahramani, S.G. Evans, S. McDougall, A. Small and W.A. Take. 2021b. *A Comprehensive Global Database of Tailings Flows.* Borealis, the Canadian Dataverse Repository. https://doi.org/10.5683/SP2/NXMXTI

Small, A., M. James and M. Al-Mamun. 2017. Advancing the state of practice for tailings dam breach assessment using empirical correlations. *Proceedings of Canadian Dam Association Annual Conference.* Kelowna, BC, Canada. October 16–18.

Takahashi, T. 2014. Chapter 7: Debris flow disasters and their reproduction by computer simulations. In *Debris Flow: Mechanics, Prediction and Countermeasures* (2nd edition, p. 572). CRC Press. Boca Raton.

USBR (US Bureau of Reclamation). 1998. Downstream Hazard Classification Guidelines. Department of the Interior.

Wahl, T.L. 1998. Prediction of Embankment Dam Breach Parameters: Literature Review and Needs Assessment., Water Resources Research Laboratory Report DSO-98-004.

Wahl, T.L. 2004. Uncertainty of Predictions of Embankment Dam Breach Parameters. *J Hydraul Eng* 130(5): 389–397.

Wahl, T.L. 2014. Evaluation of Erodibility-Based Embankment Dam Breach Equations. Water Resources Research Laboratory Report HL-2014-02.

Walder J.S. and J.E. O'Connor. 1997. Methods for predicting peak discharge of floods caused by failure of natural and constructed earthen dams. *Water Resour. Res.* 33(10): 2337–2348.

Walsh, A., S. McDougall, S.G Evans and W. A. Take. 2021. Effect of upstream dam geometry on peak discharge during overtopping breach in noncohesive homogeneous embankment dams; implications for tailings dams. *Water Resour. Res*. 57. Accessed at https://doi.org/10.1029/2020WR029358

Washington State Department of Ecology (Washington Guidelines). 2007. *Dam Safety Guidelines: Technical Note 1 Dam Break Inundation Analysis and Downstream Hazard Classification.*

Xu. Y. and L.M. Zhang. 2009. Breaching Parameters for Earth and Rockfill Dams. *J. Geotech. Geoenviron. Eng.* 135(12): 1957–1970.

Appendix

Table A1: Events used to develop equations – water retaining dams (Wahl, 2014)

Event	Height of Water above Breach invert (m)	Outflow Volume (m³)	Formation Time (h)	Eroded Dam Volume (m³)
Apishapa, USA, 1923	27.8	22,202,640	0.75	238,000
Baldwin Hills, USA, 1963	18.3	910,308	0.33	31,700
Bearwallow Lake, USA, 1976	5.8	49,300	–	1,090
Buckhaven No. 2, USA, Unknown	6.1	24,700	–	1,070
Bullock Draw Dike, USA, 1971	3.1	740,088	–	1,350
Butler, USA, 1982	7.2	2,380,000	–	4,310
Castlewood, USA, 1993	21.7	9,251,100	0.50	55,700
Caulk Lake, USA, Unknown	11.4	698,000	–	13,700
Clearwater Lake, USA, 1994	4.1	466,000	–	1,290
East Fork Pond River, USA, 1978	9.8	1,870,000	–	7,630
Elk City, USA, 1936	9.4	1,180,000	–	16,900
Emery, USA, Unknown	6.6	425,000	0.83	1,970
Euclides da Cunha, Brazil, 1977	58.3	57,973,560	–	726,000
Fogelman, USA, Unknown	11.1	493,000	–	2,050
Frankfurt, Germany, 1977	8.2	351,542	–	1,290
French Landing, USA, 1925	8.5	3,873,127	2.58	13,800
Frenchman Creek, USA, 1952	10.8	16,035,240	–	28,400
Goose Creek, USA, 1916	4.5	579,736	0.50	1,070
Grand Rapids, USA, 1900	7.5	255,000	–	1,800
Haas Pond, USA, Unknown	4	23,400	–	708
Hart, USA, 1986	10.7	6,350,000	–	24,800
Hatchtown, USA, 1914	16.8	14,800,000	1.00	161,000
Hell Hole, USA, 1964	35.1	30,590,304	0.75	555,000
Horse Creek, USA, 1914	7	12,800,000	–	20,500
Hutchinson, USA, 1994	4.4	1,170,000	–	1,750
Ireland #5, USA, 1984	3.8	160,000	0.50	1,260
Johnstown (South Fork Dam), USA, 1889	24.6	18,921,583	0.75	68,800
Johnston City, USA, 1981	3.1	574,802	–	673
Kelly Barnes, USA, 1977	11.3	777,092	–	9,940
Kraftsmen's Lake, USA, 1994	3.7	177,000	–	376
La Fruta, USA, 1930	7.9	78,900,000	–	32,900
Lake Avalon, USA, 1904	13.7	31,500,000	2.00	81,000
Lake Frances, USA, 1899	14	789,427	–	12,400
Lake Genevieve, USA, Unknown	6.7	680,000	–	2,630
Lake Latonka, USA, 1966	6.3	4,090,000	–	9,540
Lake Philema, USA, 1994	9	4,780,000	–	11,300

Lambert Lake, USA, Unknown	12.8	296,000	–	5,870
Laurel Run, USA, 1982	12.8	382,379	–	19,500
Lawn Lake, USA, 1982	6.7	798,000	–	2,400
Little Deer Creek, USA, 1963	22.9	1,360,000	0.33	50,600
Long Branch Canyon, USA, Unknown	3.2	284,000	–	378
Lower Latham, USA, 1973	5.8	7,080,000	1.50	14,300
Lower Otay, USA, 1916	39.6	49,300,000	1.00	107,000
Lyman, USA, 1915	16.2	35,770,920	–	71,900
Lynde Brook, USA, 1876	12.2	2,874,008	–	15,300
Melville, USA, 1909	7.9	24,700,000	–	10,600
Merimac Upper Lake, USA, 1994	3.4	69,600	–	758
Mossy Lake, USA, 1994	4.4	4,130,000	–	2,040
Oros, Brazil, 1960	35.4	650,043,960	8.50	765,000
Otter Lake, USA, Unknown	5	109,000	–	1,170
Potato Hill Lake, USA, 1977	7.8	105,000	–	3,010
Quail Creek, USA, 1989	16.7	30,800,000	1.00	84,400
Rainbow Lake, USA, 1986	10	6,780,000	–	10,500
Renegade Resort Lake, USA, Unknown	3.7	13,900	–	92
Rito Manzanares, USA, 1975	4.6	24,670	–	1,290
Salles Oliveira, Brazil, 1977	38.4	71,541,840	–	440,000
Schaeffer Reservoir, USA, 1921	30.5	4,440,528	0.50	227,000
Scott Farm Dam no. 2, Canada, Unknown	10.4	86,000	–	7,020
Sheep Creek, USA, 1970	14	910,000	–	18,300
Sinker Creek, USA, 1943	21.4	3,330,396	2.00	84,100
Spring Lake, USA, 1889	5.5	135,683	–	612
Statham Lake, USA, 1994	5.6	564,000	–	1,350
Teton, USA, 1976	77.4	309,603,480	1.25	3,060,000
Trial Lake, USA, Unknown	5.2	1,480,000	–	829
Trout Lake, USA, Unknown	8.5	493,000	–	4,830
Wheatland no. 1, USA, 1969	12.2	11,594,712	1.50	14,600
Wilkinson Lake, USA, 1994	3.6	533,000	–	1,420
Winston, USA, 1912	6.4	662,379	–	1,480

Table A2: Events used to develop equations – tailings storage facilities (Adria et al., 2023b)

Event	Height of Water above Breach Invert (m)	Outflow Volume (m^3)	Formation Time (h)	Eroded Dam Volume (m^3)
Aznalcóllar, Spain, 1998	26	15,000,000	2.0	150,000
MAL Reservoir X (Ajka), Hungary, 2010	21.8	1,200,000	0.25	74,000
Mount Polley, Canada, 2014	37.7	24,400,00	3.5	600,000

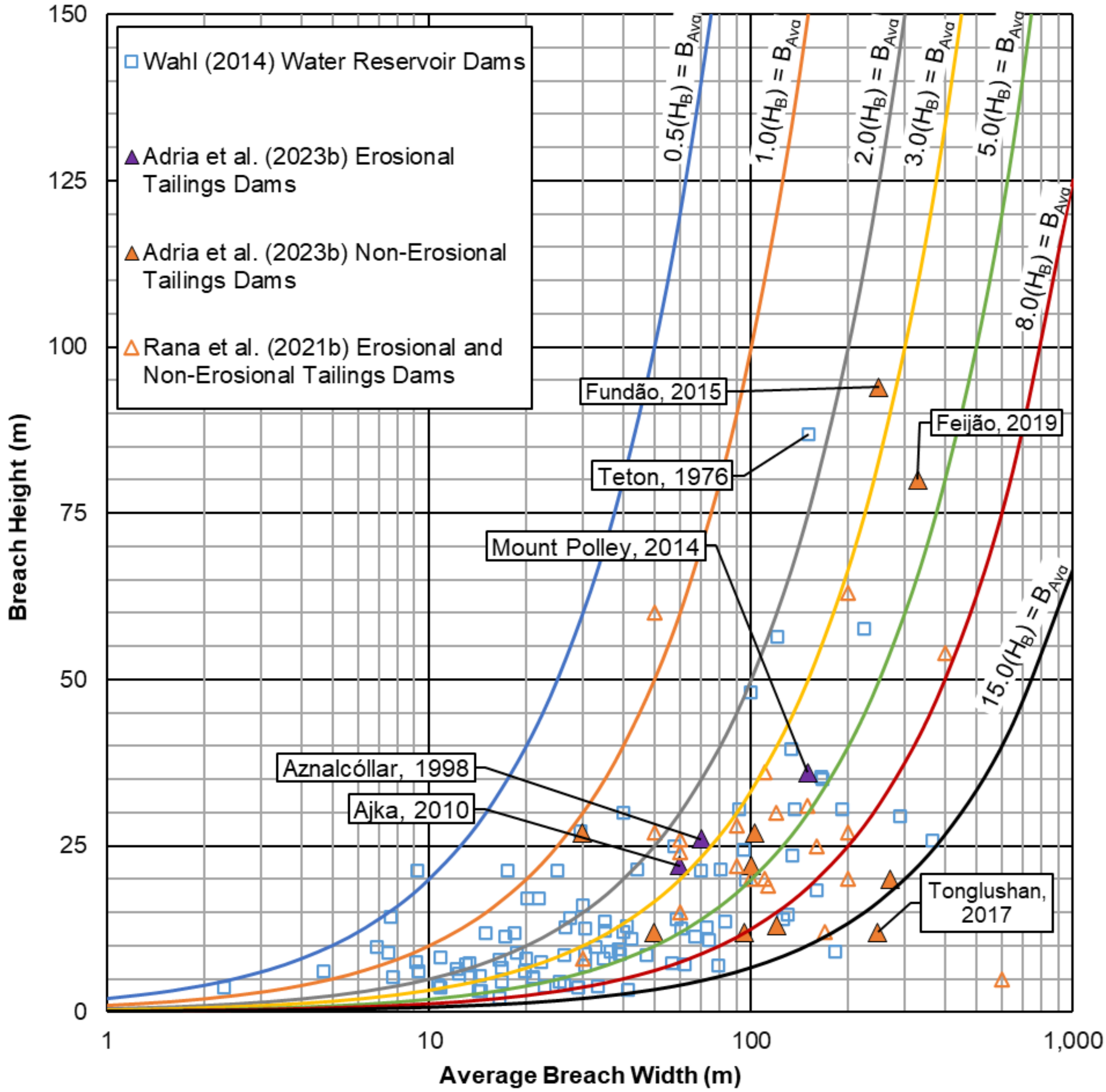

Figure A1: Breach height to breach width ratios (adapted from Wahl, 1998)

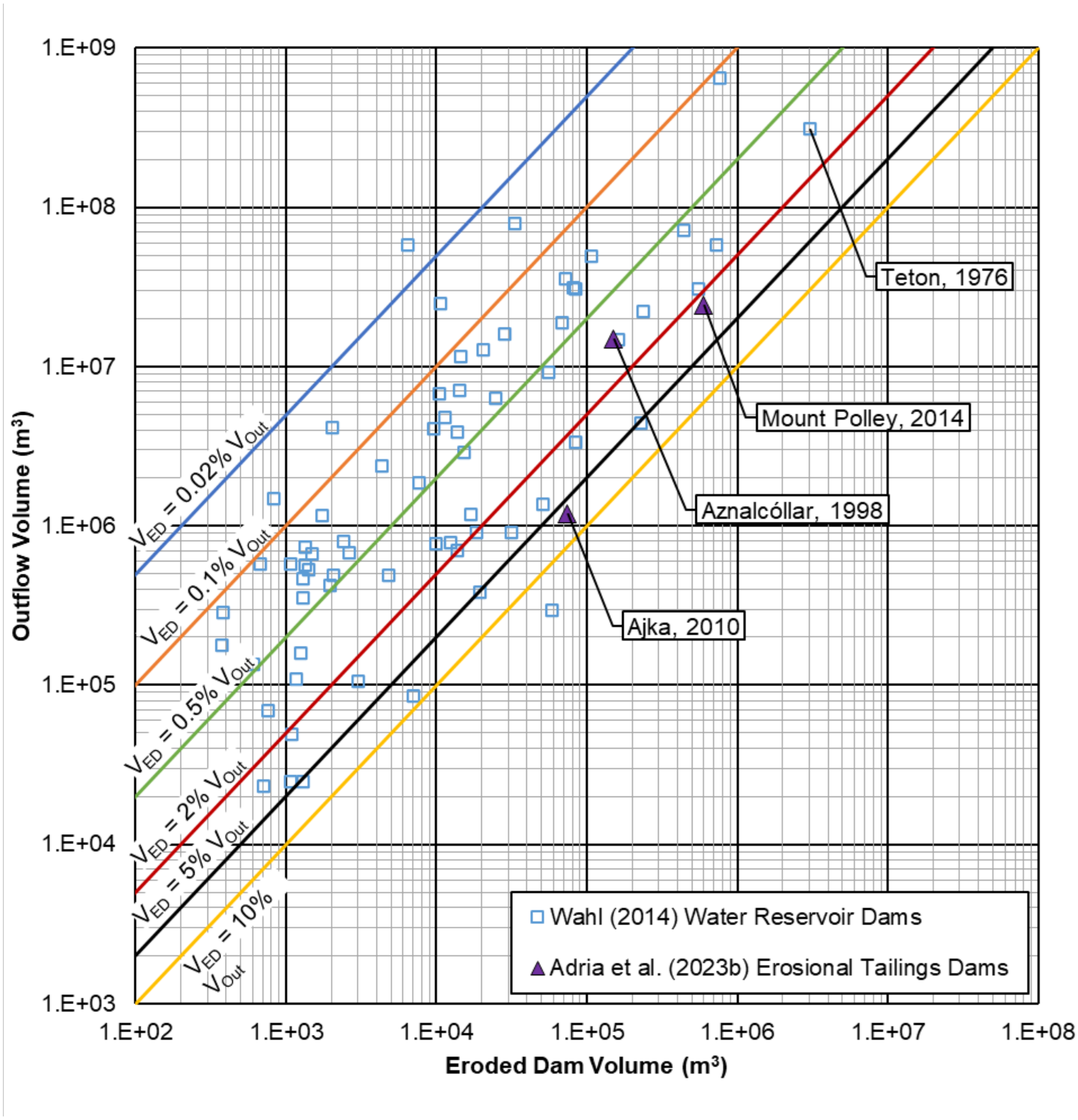

Figure A2: Outflow volume to eroded dam volume ratio

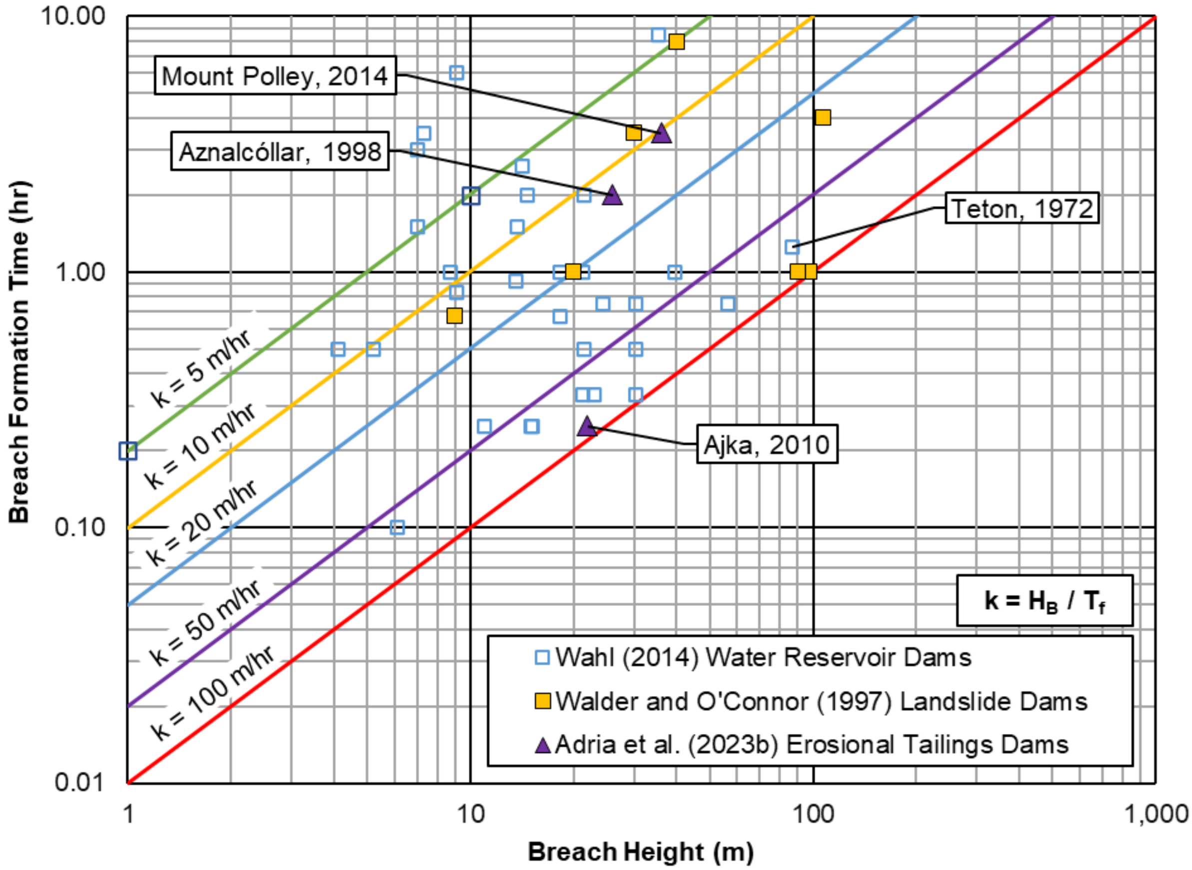

Figure A3: Mean erosion rates for various types of dam failures

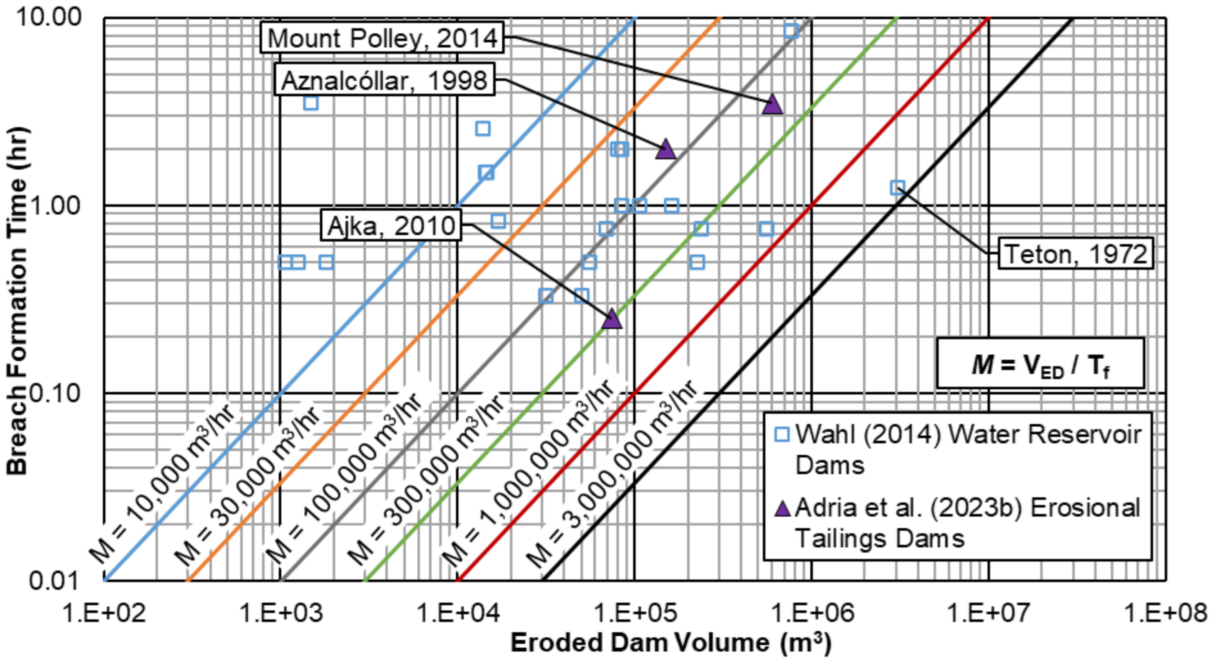

Figure A4: Mean eroded dam volume rates for various types of dam failures